COMPREHENSIVE NONDESTRUCTIVE TESTING OF IMPLANTS FOR ORTHOPEDIC APPLICATIONS

Cristina LUȚĂ[1], Marian SOARE[2], Aura-Cătălina MOCANU[1,2], Andreea MAIDANIUC[1,2], Adrian ERNUȚEANU[2], Florin MICULESCU[1*]

The aim of the study was to evaluate the perspectives of using conventional nondestructive examination methods for defects localization on orthopedic implants. Different metallic medical devices, made of 316L austenitic stainless steel, Co-Cr alloys and Ti-6Al-4V alloys, were subjected to nondestructive evaluation. Each material grade was verified by positive material identification (PMI), using portable X-ray fluorescence spectrometry (PXRF). Different flaws and defects were detected through radiographic testing (RT), liquid penetrant testing (PT) and Eddy Current testing (ET), which were performed according to standard test methods and in-house procedures.

Keywords: biomaterials, metallic implants, nondestructive examination, radiographic testing, Eddy current testing, liquid penetrant testing

1. Introduction

Surgical implants work under aggressive conditions in terms of corrosion, and mechanical loading; their failure is influenced by many factors, including design, material selection, manufacturing practice, implantation procedure, postoperative side effects, and patient's misuse [1-6].

For high performance and satisfactory reliability of metallic medical devices, great interest is dedicated to the identification of surface and internal defects prior implantation [7]. In order to avoid implants failure, defects such as inclusions, shrinkage cavities, segregations, or signs of wear, fatigue, corrosive attack, pitting, erosion-corrosion, and stress corrosion, need to be carefully identified [8]. Many of these defects occur during the manufacturing processes (such as casting, forging, rolling, welding, or heat treatment) or during service (e.g. corrosion, cracking etc.).

In industrial applications, flaw detection in metallic components is efficiently performed by means of nondestructive testing which can detect product defects without producing any damage or affecting products' usability [9].

[1] Metallic Materials Science, Physical Metallurgy Department, Faculty of Materials Science and Engineering, University POLITEHNICA of Bucharest, Romania
[2] S.C. Nuclear NDT Research & Services S.R.L, Bucharest, Romania
*corresponding author: f_miculescu@yahoo.com; florin.miculescu@gmail.com

Various nondestructive testing methods were developed, based on the specific needs of each industrial application. The medical industry, in which human safety and well-being are the primary focus, could benefit from the advantages of various methods which allow the scientists and engineers to test entire batches of samples without affecting their integrity. Various defects, such as porosities or internal voids within implants, are associated with an increased corrosion tendency and fatigue failure after implantation [6, 7], so early detection of these defects, preferably in a nondestructive manner, could contribute significantly to a successful implant evaluation.

Currently, NDT testing of medical devices is performed mostly by liquid penetrant testing (PT) and ultrasonic testing (UT). However, it is challenging to apply both methods for entire batches of medical devices [9]. In PT, a penetrant is applied on specimen surface, which is absorbed by defects opened at surface. After the penetrant is removed, a developer is applied to indicate the presence of surface defects. The developer will expose the discontinuities for visual examination [10]. The method is widely used for examination of smooth materials such as metals, glasses, plastics and ceramics used in biomedical field [11-13]. However, PT can only reveal defects which are opened to sample's surface, regardless of implants geometry. Also, the method uses many substances such as penetrants and developers and different accessories like gloves and cleaners, and since evaluation is performed on finished parts, these materials need to be carefully controlled and documented. Ultrasonic testing, although successfully used in many industries, is dependent on sample geometry and is mostly used in preliminary stages of medical device fabrication, on raw materials with simpler shapes (such as bars, blocks or plates) [9].

However, besides PT and UT, NDT testing includes a wide range of examination and testing methods. Their corroborate use in extensive testing programs could provide complementary data regarding finished parts integrity. In this study, we used PT and three other nondestructive testing methods to evaluate the integrity and composition of various metallic implants. The proposed methods are radiographic testing/ radiological testing (RT), Eddy current testing/ electromagnetic testing (ET) and positive material identification (PMI) performed with a portable x-ray fluorescence spectrometer (PXRF).

RT is a volumetric nondestructive method used for detection of internal flaws in many industrial applications [14] including evaluation of medical devices [15-17]. The method uses radiation (x-rays or gamma rays) to penetrate the material and to record flaws images on a photographic film. Some of the radiation passes through the material and is absorbed by it, while some radiation is transmitted through the less dense metal in the locations of imperfections. The radiographic results are displayed as an impression on the radiographic film; RT data are then interpreted to obtain information regarding the flaws present in the

specimen [17]. Despite its great advantages, the method cannot detect some planar defects nor indicate the depth of discontinuities. Presence of less dense metallic images on the radiographic film could also be associated with surface imperfections related to local thickness (such as local deformations or excess material) [18].

ET uses electromagnetic currents induced on the surface of examined samples. When a coil of conductive wire is excited with an alternating electrical current, it will produce an alternating magnetic field which oscillates at the same frequency as the current running through the coil. If the coil is situated near a conductive material, some currents opposed to the ones in the coil will be induced in the material. These currents are called "eddy currents". When imperfections are encountered in a sample, they will cause a perturbation in the circular flow patterns of the eddy currents and reduce their intensity. The change is recorded by ET equipment, allowing flaw detection and characterization. ET is able to detect both surface and sub-surface flaws and has many applications in chemical or petrochemical industry, aeronautical, automotive, aircraft and biomedical industries for identification of material discontinuities [19, 20].

PMI is also a nondestructive field-testing method based on X-ray fluorescence spectrometry (XRF) or optical emission spectrometry (OES), used for the compositional analysis and grade identification of various metallic and nonmetallic products. A portable XRF spectrometer is a miniaturized equipment which provides compositional results accurate enough for grade identification. The use of portable XRF analyzers for archaeological [21], environmental [22] or forensic [23] applications was already documented. However, few details are available regarding positive material identification of medical grade materials, as noted by other researchers [24-29].

Currently, metallic biomaterials are extensively used to manufacture surgical implants primarily for their mechanical properties and high corrosion resistance. The most used metallic implants in orthopedic surgery are low-carbon austenitic stainless steels (such as 316L), titanium and its alloys (Ti6Al4V or NiTi with shape memory alloy), and cobalt-chromium based alloys (Co-Cr-Mo, Co-Ni-Cr-Mo, etc.). While each material type has its own advantages, the ideal alloy should probably have the strength of cobalt–chromium alloys, the corrosion resistance and biocompatibility of titanium, and the fabrication cost of stainless steels [6].

This study aims to correlate the findings of RT, PT and ET methods for a comprehensive nondestructive characterization of metallic implants used for orthopedic applications. Eighteen implants, made of different alloys were selected for this evaluation. The present study was designed for evaluating the performance of nondestructive testing methods and correlating their results. Since the study does not aim to perform a quality control of the selected samples we

provided only partial photographs of the samples and we did not reveal the name of the device manufacturers.

2. Materials and methods

2.1. Materials

Various orthopedic implants were selected from three categories of metallic materials: stainless steel, cobalt based alloys and titanium-based alloys. Table 1 and Fig. 1 summarize the data for eighteen different metallic implants:

Table 1

Samples description and codification

Sample code	Description	Material	Surface finish
2	Acetabular cup of hip implant	Co-Cr-Mo	Porous coating
3	Femoral head of hip implant	Co-Cr-Mo	Polished
4	Femoral head of hip implant	Co-Ni-Cr-Mo	Polished
5	Femoral head of hip implant	Co-Cr-Mo	Polished
6	Femoral stem of hip implant	Ti-6Al-4V	Grit blasting
7	Femoral stem of hip implant	Co-Ni-Cr-Mo	Milled
8	Total hip endoprosthesis	316 L	Milled
9	Tibial component of knee implant	Ti-6Al-4V	Milled
10	Tibial component of knee implant	Ti-6Al-4V	Milled
11	Femoral component of knee implant	Co-Cr-Mo	Polished
12	Tibial component of knee implant	Ti-6Al-4V	Milled
13	Total knee endoprosthesis	Co-Cr-Mo	Milled
14	Total knee endoprosthesis	Co-Cr-Mo	Polished
15	Intramedullary stem	316 L	Polished
16	Flexible intramedullary nail	316 L	Polished
17 A	Screw for fixing the intramedullary stems	316 L	Grinded
17 B	Screw for fixing the intramedullary stems	316 L	Grinded
18	Tibial Nail	316 L	Polished

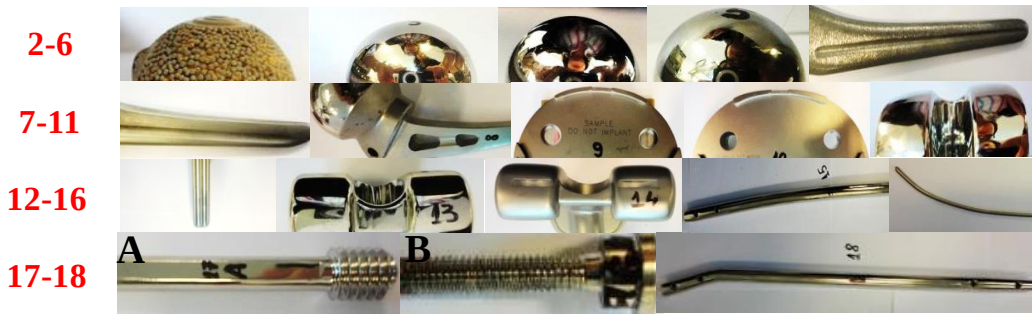

Fig.1. Metallic implants included in the current study

2.2. Methods

Material identification of the metallic implants was performed in accordance with ASTM E1476 requirements [30], with a portable X-ray fluorescence spectrometer (SPECTRO xSORT Handheld). The samples were analyzed in their as-received state, without further preparation. The PMI results represent the average of three measurements performed in repeatability conditions, following a validated working procedure. The measurement uncertainty was estimated as ±10% of the measured concentration.

Radiographic Testing (RT) was performed in accordance with ASTM F629 requirements [31]. RT examination was performed with X-ray at 120-150 kV energy and 4.5 mA intensity, with 700 mm maximum distance between the radiation source and the film, and 3-8 minutes exposure time. Films interpretation was performed in a dark room with a negatoscope which provided uniform illumination in the screen area.

Liquid Penetrant Testing (PT) was performed in accordance with ASTM E165/E165M requirements [32] with: *a)* Sherwin Babb Co DP-55 Penetrant; *b)* Sherwin Babb Co N-120 or DR-60 Solvent, and *c)* Sherwin Babb Co D-100 Developer. The penetrant was applied on the implant surface being maintained for 8-10 min to penetrate into flaws under the action of capillary forces. The penetrant liquid in excess was washed an aqueous solution with 5% soda ash content. The samples surface was further coated with a thin layer of developer (a kaolin suspension in water - about 500g of kaolin per 1 liter of water). Samples were dried in hot air, allowing the liquid that emerged from the defects of the specimen to color the developer in red. In this way the shape of defects appeared very clearly. The implants surface was examined twice from the moment of developer application, after 3 - 4 min (for relatively big flaws), and after 20 - 30 min (to reveal fine flaws).

Eddy Current Testing (ET) was performed in accordance with ISO 15549 requirements [33], using a NORTEC 500D Olympus instrument, equipped with: EddyMaster ET software acquisition, a surface ET probe for assessing defects and a calibration standard. A frequency of 100 kHz was selected to achieve enough deep penetration, with a gain of approximately 63 dB. A stainless-steel calibration block was used for all examined samples. This calibration block contains three rectangular notches at depths of 0.5 mm, 1 mm, and 2 mm respectively, each being of 0.15 mm wide.

3. Results and discussion

3.1. Positive Material Identification – PMI-XRF

The compositional results obtained by X-ray fluorescence (XRF) analysis for the eighteen metallic implants are listed in Tables 2-4. The results are

presented in comparison with standard material specifications for metallic implants. Each type of material was evaluated separately.

Ti-based alloys are suitable as biomaterials due to a moderate modulus, a low density and a good corrosion resistance [3]. Titanium alloys, especially Ti6Al4V are among the most widely used materials for medical implants [34]. The composition of Ti-based hip and knee implants, presented in Table 2, closely correspond to the UNS R56400 material specification (medical grade of Ti6Al4V alloy). However, the alloy has a possible toxic effect resulting from released vanadium and aluminum [35].

Table 2

Chemical composition of Ti6Al4V alloys

Sample code	Ti %	Al %	V %	Fe %
6 - Hip implant – stem	76.9	**11.9**	3.88	0.32
9 – Knee implant - tibial	88.0	4.09	4.12	0.15
10– Knee implant - tibial	89.8	5.03	3.84	0.17
12– Knee implant - tibial	89.1	6.44	3.76	0.19
UNS R56400 (Ti6Al4V) acc. to ASTM F1472 [31]	***Balance***	***5.50-6.75***	***3.50-4.50***	***Max. 0.30***

For the femoral component of Ti-based hip implant marked with 6 (Table 2), a concentration 11.9 % Al was identified. This result is highly different from the upper limit for Al concentration in the UNS R56400 specification (ASTM F1472) [36]. The probable cause is a contamination with alumina particles from the grit blasting used for surface preparation. Grit blasting is generally employed for descaling and surface roughening of commercial implants to increase the surface area of the implant for better osseointegration [37]. However, the rougher surface also encourages the retaining of alumina particles on the metallic surface, as previously noted [38]. The chemical composition of the steel implants (Table 3) corresponds to material specifications for 316L grade, versus *UNS S31673* specification for bars and wires (as in ASTM F138 standard specification [39]).

Table 3

Chemical composition of 316 L stainless steels

Sample code	Fe %	Mn %	Cr %	Mo %	Ni %
8 - Total hip prosthesis*	62.8	1.92	16.8	2.39	13.9
15 - Intramedullary stem	68.2	1.08	16.5	**1.93**	**9.9**
16 - Flexible intramedullary nail	63.8	1.80	17.0	2.46	13.3
17A - Screw for sample 15	68.8	1.68	16.6	**1.86**	**10.0**
18 - Tibial nail	67.8	1.93	17.2	**1.77**	**10.8**
UNS S31673 (316L) acc. to ASTM F138 [39]	***Remainder***	***Max. 2.00***	***17.0-19.0***	***2.25-3.00***	***13.0-15.0***

**analysis performed on the femoral part*

316 L austenitic stainless steel contains 17-19% Cr, 13-15% Ni and a low carbon content (maximum 0.03%). Chromium and nickel influence both the microstructure and the surface properties. Chromium, an essential element in this type of stainless steel, contributes to formation of a corrosion-resistant chromium oxide (Cr_2O_3). This surface layer has high adherence on the metallic surface, promoting self-healing in the presence of oxygen. However, due to the release of ions that can favor infections and allergies, 316 stainless steel implants are used in the body as short-term implants or as coated implants [40].

Within the composition of the intramedullary stem, the screw for intramedullary stem and the tibial nail coded in Table 3 as 15, 17 and 18 respectively, the Mo and Ni concentrations did not fit the material specification for the *UNS S31673* implant grade. However, different types of 316L steel are currently used for surgical instruments and implants fabrication; examples include the *UNS S31675* (ASTM F1586 [41]), a wrought nitrogen strengthened 21 Chromium – 10 Nickel – 3 Manganese – 2.5 Molybdenum stainless steel alloy bar for surgical implants and *UNS S20910*, a wrought nitrogen strengthened 22 Chromium – 13 Nickel – 5 Manganese – 2.5 Molybdenum stainless steel alloy bar and wire for surgical implants (ASTM F1314 [42]). Moreover, for various implant manufacturing methods, different material grades may be suitable. In Table 3, the Mo and Ni concentrations for samples 15, 17 and 18 indicate that the material is a commercial grade of 316L, usually used for surgical instruments [43].

The compositional analysis for most Co-Cr-based implants (Table 4) revealed that the samples were manufactured using a Co-Cr-Mo alloy which fits the *UNS R30075* specification for Cobalt – 28 Chromium – 6 Molybdenum casting alloys for surgical implants [44]. The PMI-XRF analysis of two implants, a femoral head of a hip implant and a femoral stem of hip implant (codes 4 and 7, respectively), revealed a composition that fits the *UNS R30035* specification, for a wrought 35 Cobalt – 35 Nickel – 20 Chromium – 10 Molybdenum alloys for surgical implant applications [45]. For the total knee implant coded 14 (femoral part was analyzed), the Cr and Co concentrations were slightly below the material specification limits. However, for this implant, the XRF analysis revealed an Al concentration of 10.7% on the implants surface, presumably due to manufacturing process that encourages the retaining of alumina particles.

Table 4

Chemical composition of Co-Cr-Mo and Co-Ni-Cr-Mo alloys

Sample code	Co %	Cr %	Mo %	Si %	Mn %	Ni %	Fe %	Ti %
				Co-Cr-Mo alloys				
2 - Hip implant – acetabular cup*	64.3	28.9	5.53	0.50	0.33	0.47	0.20	0.01
3 – Hip implant - femoral	65.4	27.0	6.00	0.45	0.66	0.17	0.09	0.04
5 – Hip implant - femoral	64.5	28.1	5.37	0.86	0.71	0.16	0.16	0.04
11 – Knee implant – femoral	64.3	27.1	5.93	0.79	0.26	0.16	0.17	0.13

13 – Knee implant – total [1]	64.8	27.6	6.03	0.91	0.40	0.15	0.06	0.03
14- Knee implant – total [1,2]	**55.9**	**25.4**	5.01	0.26	0.45	0.15	0.24	0.04
UNS R30075 acc. to ASTM F75 [44]	***Rest***	***27.0-30.0***	***5.0-7.0***	***Max. 1.00***	***Max. 1.00***	***Max. 0.50***	***Max. 0.75***	***Max. 0.10***
			Co-Ni-Cr-Mo alloys					
4 – Hip implant – head	32.2	19.2	9.53	0.16	0.16	37.0	0.38	0.64
7 –Hip implant – stem	30.5	19.2	9.72	0.17	0.13	34.5	0.24	0.83
UNS R30035 acc. to ASTM F562[45]	***Rest***	***19.0-21.0***	***9.0-10.5***	***Max. 0.15***	***Max. 0.15***	***33.0-37.0***	***Max. 1.00***	***Max. 1.00***

[1] *analysis performed on the femoral part*
[2] *Al% = 10.7*
**analysis performed in a non-porous area*

3.2. Nondestructive examination - RT, PT and ET

RT examinations revealed minor defects on six implants, illustrated in Fig. 2. The RT indications are characteristic for structural imperfections, voids and inclusions. Blow voids appeared as rounded cavities of a spherical, elongated or flattened shape while nonmetallic inclusions appeared as darker indications on the radiograph (best observed in the results for sample 8 – Fig. 2).

The tibial component of Ti6Al4V knee implant (code 12) has structural imperfections on the surface. These discontinuities are usually related to the various manufacturing processes such as machining, forming, extruding, rolling, welding, and plating [18]. In this case, the milling process may be a cause for the occurrence of detected imperfections.

the immediate vicinity of the void; similar defects were reported to be caused by insufficient gas and air discharge or insufficient permeability during fabrication and can be avoided by the proper use of equipment and foundry practice [6]. A denser inclusion (with a diameter of 1.5 mm) and an edge indication (10 mm length) were also identified in this sample, close to the access-hole (Fig. 2 – sample 8); in metallic materials, various chemical reactions, physical effects, and contamination that occur during fabrication processes are considered the main causes of inclusions [7]. Since all these defects relate with the lack of homogeneity in the casting, they are a deviation (nonconformance) of the compactness of the sample.

In the Co-Cr implants, RT examination revealed: *(i)* structural imperfections in a femoral head of the hip implant (code 5); *(ii)* low density areas in the large thickness part on the femoral component of the hip implant (code 7); *(iii)* structural imperfections on the femoral component of the knee implant (code 11), and *(iv)* a linear indication with a length of l = 5 mm on the femoral part of the total knee implant (code 13).

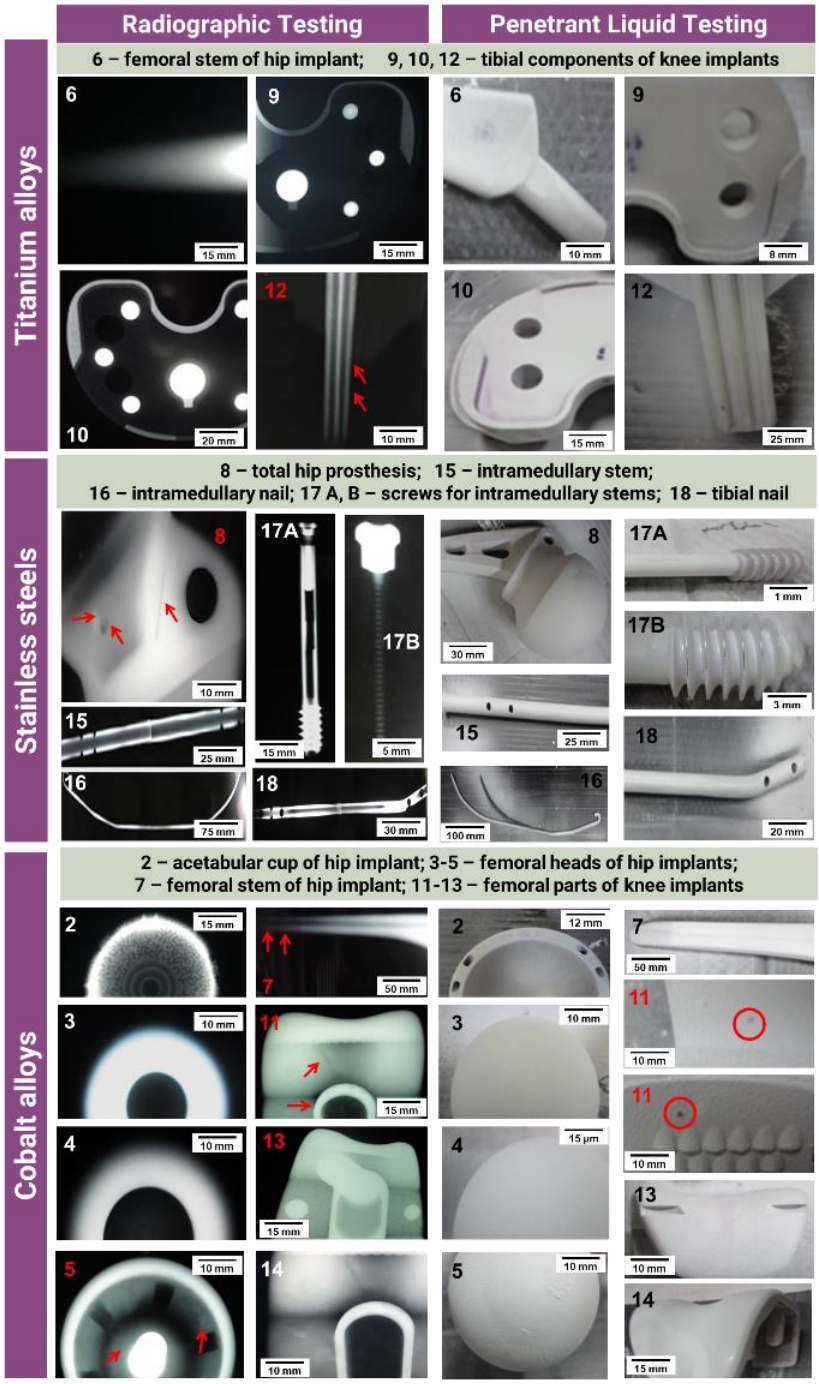

Fig.2. Representative Radiographic Testing (RT) and
Liquid Penetrant Testing (PT) results; the arrows indicate the defects position

The high degree of surface finishing of most of the metallic implants from this study makes PT very relevant and reliable for these components, considering that the roughness of the samples may affect the sensitivity of the testing method (surface preparation of the tested part is recommended if mechanical operations such as machining, sanding, or grit blasting have been performed during fabrication [47, 48]).

However, since surface preparation may lead to decrease or closing of defect's opening [48] and since we did not want to affect the integrity of the tested samples, the samples with obviously high surface roughness/porous coatings (Fig. 1) were tested without surface preparation. These samples were an acetabular cup of a hip implant (code 2) and a screw for fixing intramedullary stems (code 17B). PT results for these samples 2 and 17B have only informative purpose.

PT examinations revealed very small zones of discontinuities on the inner side of the Co-Cr femoral component of the knee implant (code 11). We note that for the same implant, RT examination revealed surface irregularities and local deformations (Fig. 2).

In the femoral area of total hip implant (code 8), RT examinations revealed an elliptical void of approximately 3 × 4 mm and a metallic inclusion in

No critical flaws, such as cracks or porosities were noted for the rest of metallic implants.

Eddy current examinations (ET) were performed only on the samples that did not show porosities and had a smooth surface (implants 2 and 17B were excluded). Two kinds of defects were identified by ET examinations: cracks and near surface defects. Fig. 3 shows the impedance plan responses during ET, the vertical signal component corresponding to the indications produced by sample imperfections; a surface coil probe at frequency of 100 kHz was used for sample scanning.

ET data (Fig. 3) revealed defects for five implants: *(1)* a scratch in the edge area on the Ti6Al4V tibial component of the knee implant (code 9), for which no defects were revealed in the previous examinations, *(2)* three discontinuities on the femoral part of the 316 L total hip implant (code 8), *(3)* a structural imperfection on the Co-Cr femoral head of the knee implant (code 5), *(4)* a surface imperfection on the peak area of the Co-Cr femoral component of the hip implant (code 7), also identified by RT examinations and *(5)* two discontinuities on the inner side of the Co-Cr femoral component of knee implant (code 11) also detected by the PT examinations.

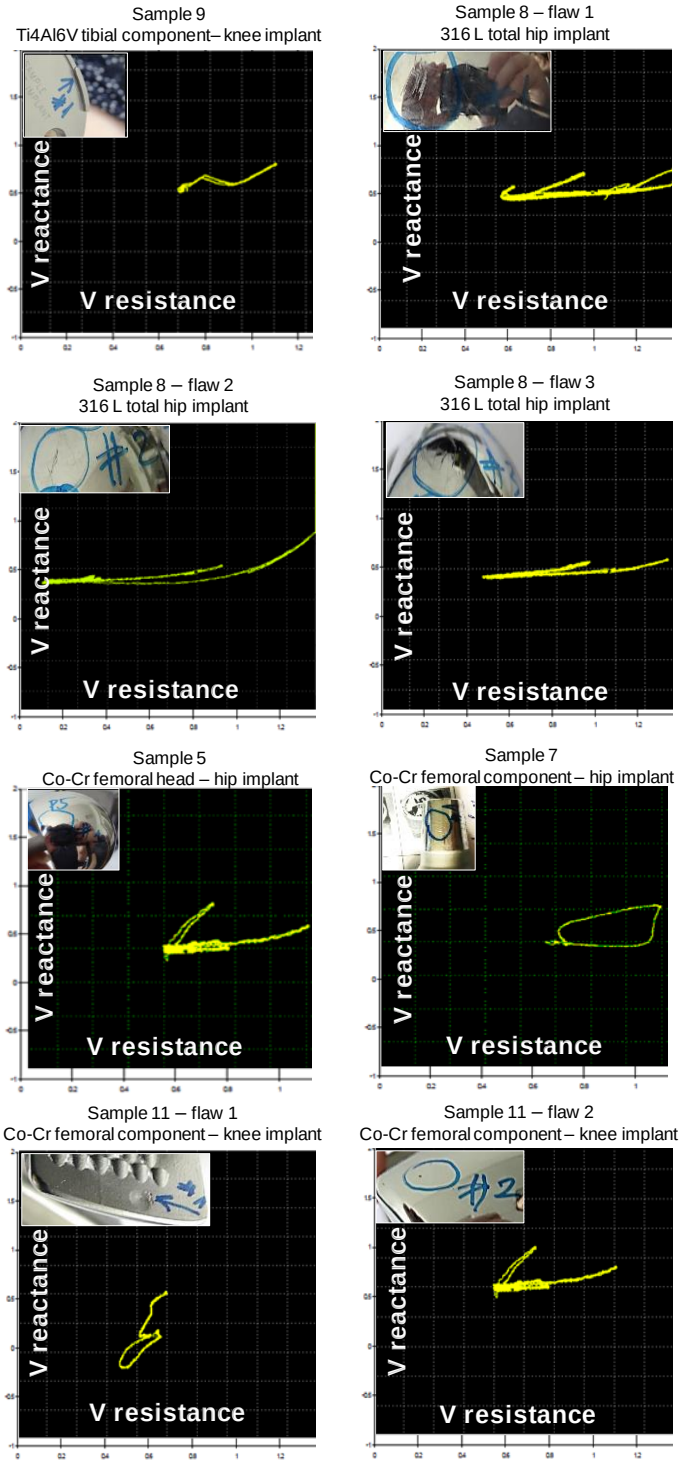

Fig. 3. Representative Eddy Current (ET)
flaw signals in the impedance plane presentation

The results obtained by radiographic testing, liquid penetrant testing and Eddy current testing are compared in Table 5. The main observations are:

- RT identified defects in 6 samples and ET identified defects in 5 samples (not the same samples). Only some minor discontinuities were detected by PT examination;
- For sample 11 (femoral component of Co-Cr knee implant), all three methods identified imperfections. PT and ET results correlate closely, since both identified discontinuities on the surface and near-surface of the sample;
- For samples 7 (femoral component of Co-Ni hip implant) and 8 (316L total hip prosthesis) both RT and ET identified imperfections. However, the data provided by the testing methods did not lead to the same results. For the femoral component of the hip implant, RT could differentiate between the void and inclusions, while ET testing identified all defects as discontinuities. In the second case, the total hip prosthesis, RT identified an area with low density associated to a surface imperfection, while ET identified additional discontinuities.
- For samples 5, 6 (femoral components of hip implants), 9, 12 (tibial components of knee implants), and 13 (total knee implant) only one nondestructive testing method identified defects, which enforce the need for complementary nondestructive evaluation.

4. Conclusions

This study evaluated the perspectives of combining complementary non-destructive testing methods widely used in industrial applications (radiographic testing, liquid penetrant testing and Eddy current testing) for examining metallic implants for orthopedic applications. Eighteen implants manufactured from Ti-based alloys, Co-Cr alloys and stainless steel were subjected to the non-destructive evaluation. Grade identification was performed by positive material identification with a portable X-ray fluorescence spectrometer. The results provided by the equipment allowed the identification of different standard (ASTM) grades of metallic alloys for surgical implants.

Table 5

Comparison between RT, PT and ET results

Code	Description	Material	Surface finish	RT	PT	ET
2	Acetabular cup of hip implant	Co-Cr-Mo	Porous coating	-	-	*Not suitable*
3	Femoral head of hip implant	Co-Cr-Mo	Polished	-	-	-
4	Femoral head of hip implant	Co-Ni-Cr-Mo	Polished	-	-	-

Code	Description	Material	Surface finish	RT	PT	ET
5	Femoral head of hip implant	Co-Cr-Mo	Polished	Structural irregularities	-	-
6	Femoral stem of hip implant	Ti-6Al-4V	Grit blasting	-	-	Structural imperfections
7	Femoral stem of hip implant	Co-Ni-Cr-Mo	Milled	Low density in the large thickness area	-	Surface imperfection
8	Total hip endoprosthesis	316 L	Milled	Elliptical void + 2 inclusions	-	Three discontinuities
9	Tibial component of knee implant	Ti-6Al-4V	Milled	-	-	Scratch in the edge area
10	Tibial component of knee implant	Ti-6Al-4V	Milled	-	-	-
11	Femoral component of knee implant	Co-Cr-Mo	Polished	Irregularities and superficial deformation	Discontinuities on the inner side	Two discontinuities on the inner side
12	Tibial component of knee implant	Ti-6Al-4V	Milled	Structural irregularities on the surface	-	-
13	Total knee endorosthesis	Co-Cr-Mo	Polished	Linear indication	-	-
14	Total knee endoprosthesis	Co-Cr-Mo	Milled	-	-	-
15	Intramedullary stem	316 L	Polished	-	-	-
16	Flexible intramedullary nail	316 L	Polished	-	-	-
17 A	Screw for fixing intramedullary stems	316 L	Grinded	-	-	-
17 B	Screw for fixing intramedullary stems	316 L	Grinded	-	-	*Not suitable*
18	Tibial Nail	316 L	Polished	-	-	-

Radiographic and Eddy current testing identified the majority of imperfections within the metallic implants. Different discontinuities, such as inclusions, voids, local deformations or scratches were identified. Similar defects were identified by both RT and ET results only for a single sample from the testing lot. For the other samples, the non-destructive testing results confirmed the need for extensive evaluation by means of complementary techniques to achieve a higher level of quality control adequate for medical applications. This work is particularly relevant in terms of the high detection capability of imperfections by RT, PT and ET non-destructive testing methods. Evaluating the indications obtained by these methods to accept or reject the detected imperfections is an important objective for the future work in the field of non-destructive examinations of metallic implants, in order to substantiate a real quality control of these products.

Acknowledgement

This work was supported by a grant of the Romanian National Authority for Scientific Research and Innovation, CNCS – UEFISCDI, project number PN-III-P2-2.1-PED-2016-0892.

Authors are thankful to the technical personnel of Nuclear NDT Research & Services laboratories for performing the nondestructive examinations.

R E F E R E N C E S

[1]. *D.F. Williams,* "A review of metallurgical failure modes in orthopedic implants", Retrieval and analysis of orthopaedic implants: proceedings of a symposium held at the National Bureau of Standards, Gaithersburg, Maryland, pp. 11-21, 1977

[2]. *F. Miculescu, I. Jepu, C.P. Lungu, M. Miculescu, M. Bane*, "Researches Regarding the Microanalysis Results Optimisation on Multilayer Nanostructures Investigations", Digest Journal of Nanomaterials and Biostructures, **vol. 6**, no. 2, 201, pp. 769-778.

[3]. *F. Miculescu, D. Bojin, L.T. Ciocan, I.A. Antoniac, M. Miculescu, N. Miculescu,* "Experimental Researches on Biomaterial-Tissue Interface Interactions", Journal of Optoelectronics and Advanced Materials, **vol. 9**, no. 11, 2007, pp. 3303-3306.

[4]. *C.R.F. Azevedo, E. Hippert Jr,* "Failure analysis of surgical implants in Brazil". Engineering Failure Analysis, **vol. 9**, no.6, 2002, pp.621-633.

[5]. *F. Miculescu, A. Maidaniuc, SI. Voicu, VK. Thakur, GE. Stan, LT. Ciocan*, Progress in Hydroxyapatite-Starch Based Sustainable Biomaterials for Biomedical Bone Substitution Applications, ACS Sustainable Chemistry & Engineering, **vol. 5**, no. 10, 2017, pp. 8491-8512.

[6]. *J.R. Davis,* Handbook of Materials for Medical Devices, ASM International, Metal Parks, Ohio, 2003.

[7]. *L. Patisano, L. Trojman, M. Aoulaiche, R. O'Connor, B. Kaczer, G. Groeseneken* "Understanding and Importance of Defects in Advanced Materials", ECS Transactions, **vol. 18**, no. 1, Mar. 2009, pp. 651-658.

[8]. *B. Aksakal, Ö. S. Yildirim, H. Gul,* "Metallurgical failure analysis of various implant materials used in orthopedic applications", in Journal of Failure Analysis and Prevention, **vol. 4**, no.3, June 2009, pp. 17–23.

[9]. *R. Goodwin, P. Trach*, "Nondestructive testing of implanted medical device materials: detecting defects in medical devices before they are implanted is critical to ensure the safety and reliability of such devices" in Quality, **vol. 56**, no. 4, Apr. 2017, pp.A15-A15.

[10]. *P. Dias, K. Sukasam, J. H. Jin, A. A. Khan*, Eddy Current Testing at Level 2: Manual for the Syllabi Contained IAEA-TECDOC-628/Rev.2 'Training Guidelines for Non-Destructive Testing Techniques, International Atomic Energy Agency, Vienna, 2011.

[11]. *R. Singh*, Applied Welding Engineering: Processes, Codes, and Standards, Butterworth-Heinemann, Oxford, 2015.

[12]. *H. Fischer, F. Karaca, R. Marx*, Detection of microscopic cracks in dental ceramic materials by fluorescent penetrant method, in Journal of Biomedical Materials Research Part A, **vol. 61**, no.1, 2002, pp. 153-158.

[13]. *M. Karl, Matthias, H. Fischer, F. Graef, M.G. Wichmann, T.D. Taylor, S. M. Heckmann*, "Structural changes in ceramic veneered three-unit implant-supported restorations as a consequence of static and dynamic loading." In Dental materials, **vol. 24**, no. 4, 2008, pp. 464-470.

[14]. *R. Crane,* "Radiographic Inspection of Composite Materials", in Comprehensive Composite Materials II, Elsevier, Oxford, 2018 (available online at https://doi.org/10.1016/B978-0-12-803581-8.03928-X).
[15]. *B.T. Cecconi, G. K. Raymond, D. P Rodney, M. L. Cecconi*, "Casting titanium partial denture frameworks: a radiographic evaluation", in Journal of Prosthetic Dentistry, **vol. 87**, no. 3, 2002, pp. 277-280.
[16]. *D. Dharmar, R.J. Rathnasamy, T.N. Swaminathan*, "Radiographic and metallographic evaluation of porosity defects and grain structure of cast chromium cobalt removable partial dentures." in Journal of Prosthetic Dentistry, **vol. 69**, no. 4, 1993, pp. 369-373
[17]. *I. J. Pesun, F.M. Gardner*, "Fabrication of a guide for radiographic evaluation and surgical placement of implants", in Journal of Prosthetic Dentistry, **vol. 73**, no. 6, 1995, pp. 548-552
[18]. *A.A. Khan, A.N. bin Ibrahim, G. Singh*, Ultrasonic Testing of Materials at Level 2:Training Manual for Nondestructive Testing Techniques, International Atomic Energy Agency, Vienna, 1999.
[19]. *K.A Reddy*, "Non-Destructive Testing, Evaluation Of Stainless Steel Materials", in Materials Today: Proceedings, **vol. 4**, no. 8, Oct. 2017, pp. 7302–7312.
[20]. *H. Brauer, M. Ziolkowski, H. Toepfer*, "Defect Detection in Conducting Materials Using Eddy Current Testing Techniques", in Serbian Journal of Electrical Engineering, **vol. 11**, no. 4, Dec. 2014, pp. 535-549.
[21]. *Christensen, M. A. Smith, and R. M. Thomas* "Validation of X-Ray Fluorescence Spectrometry for Determining Osseous or Dental Origin of Unknown Material" in Journal of forensic sciences, **vol. 57**, no. 1, Jan. 2012, pp. 47-51.
[22]. *M. J. Clinton, C.S. Clark, J.A. Deddens, K. Ashley, S. Roda* "Evaluation of a portable X-ray fluorescence instrument for the determination of lead in workplace air samples." in Applied occupational and environmental hygiene, **vol. 14**, no. 5, Jan.1999, pp. 306-316.
[23]. *C. Vanhoof, V. Corthouts, and K. Tirez* "Energy-dispersive X-ray fluorescence systems as analytical tool for assessment of contaminated soils "in Journal of Environmental Monitoring, **vol. 6**, no. 4, 2004, pp. 344-350.
[24]. *P. T. Palmer, R. Jacobs, P.E. Baker, K. Ferguson, S. Webber*, "Use of Field-Portable XRF Analyzers for Rapid Screening of Toxic Elements in FDA-Regulated Products" in Journal of Agricultural and Food Chemistry, **vol. 57,** no. 7, 2009, pp. 2605-2613
[25] *F. Miculescu, A.C. Mocanu, G.E. Stan, M. Miculescu, A. Maidaniuc, A. Cîmpean, V. Mitran, S.I. Voicu, T. Machedon-Pisu, L.T. Ciocan*, "Influence of the modulated two-step synthesis of biogenic hydroxyapatite on biomimetic products' surface", Applied Surface Science, **vol. 438**, 2018, pp. 147-157.
[26] *A. Maidaniuc, F. Miculescu, S.I. Voicu, C. Andronescu, M. Miculescu, E. Matei, A.C. Mocanu, I. Pencea, I. Csaki, T. Machedon-Pisu, L.T. Ciocan*, "Induced wettability and surface-volume correlation of composition for bovine bone derived hydroxyapatite particles", Applied Surface Science, **vol. 438**, 2018, pag. 158-166.
[27] *F. Miculescu, A.C. Mocanu, C.A. Dascalu , A. Maidaniuc, D. Batalu, A. Berbecaru, S.I. Voicu, M. Miculescu, V. Kumar Thakur, L.T. Ciocan*, "Facile synthesis and characterization of hydroxyapatite particles for high value nanocomposites and biomaterials", Vacuum, **vol. 146**, 2017, pag. 614-622.
[28] *A. Maidaniuc, M. Miculescu, S.I. Voicu, L.T. Ciocan, M. Niculescu, M.C. Corobea, M.E. Rada, F. Miculescu*, "Effect of micron sized silver particles concentration on the adhesion induced by sintering and antibacterial properties of hydroxyapatite microcomposites", Journal of Adhesion Science and Technology, **vol. 30**, No. 17, 2016, pp. 1829-1841.
[29] *F. Miculescu, L.T. Ciocan, M. Miculescu, A. Ernuteanu,* "Effect of Heating Process on Micro Structure Level of Cortical Bone Prepared for Compositional Analysis", Digest Journal of Nanomaterials and Biostructures, **vol. 6**, No. 1, 2011, pp. 225-233.

[30]. ASTM E1476-04 (2014) - Standard Guide for Metals Identification, Grade Verification and Sorting.
[31]. ASTM F629-15 - Standard practice for Radiography of Cast Metallic Surgical Implants.
[32]. ASTM E165/E165M-12 - Standard Practice for Liquid Penetrant Examination for General Industry
[33]. ISO 15549:2008 - Non-destructive testing - Eddy current testing - General principles.
[34]. *M. Balažic, J. Kopać*, "Machining of Titanium Alloy Ti-6Al-4V for Biomedical Applications", in Journal of Mechanical Engineering, **vol. 56**, no.3, Mar.2010, pp. 202-216.
[35]. *C. N. Elias, J. H. C. Lima, R. Valiev, M. A. Meyers*, "Biomedical applications of titanium and its alloys", in Journal of The Minerals, Metals & Materials Society, **vol. 60**, no. 3, Mar. 2008, pp. 46–49.
[36]. ASTM F1472-14, Standard Specification for Wrought Titanium-6Aluminum-4Vanadium Alloy for Surgical Implant Applications.
[37]. *J. E. Ellingsen, P. Thomsen, S. P. Lyngstadaas*, "Advances in dental materials and tissue regeneration", in Periodontology 2000, **vol. 41**, no. 1, Jun. 2006, pp. 136-156.
[38]. *A. Wennerberg, T. Albrektsson*, "Effects of titanium surface topography on bone integration - a systematic review", in Clinical Oral Implants Research, **vol. 20**, no. s4, Sept. 2009, pp. 172-184.
[39]. ASTM F138-13a, Standard Specification for Wrought 18Chromium-14Nickel-2.5Molybdenum Stainless Steel Bar and Wire for Surgical Implants.
[40]. *M. Prakasam, J. Locs, K. Salma-Ancane, D. Loca, A. Largeteau, L. Berzina-Cimdina*, "Biodegradable Materials and Metallic Implants—A Review", in Journal of Functional Biomaterials, **vol. 8**, no. 4, Sept 2017, p.44
[41]. ASTM F1586-13e1 - Standard Specification for Wrought Nitrogen Strengthened21Chromium- 10Nickel-3Manganese-2.5Molybdenum Stainless Steel Alloy Bar for Surgical Implants (UNS S31675).
[42]. ASTM F1314-13ae1 - Standard Specification for Wrought Nitrogen Strengthened 22 Chromium–13 Nickel–5 Manganese–2.5 Molybdenum Stainless Steel Alloy Bar and Wire for Surgical Implants (UNS S20910).
[43]. ASTM F899-12b - Standard Specification for Wrought Stainless Steels for Surgical Instruments.
[44]. ASTM F75-12 - Standard Specification for Cobalt-28 Chromium-6 Molybdenum Alloy Castings and Casting Alloy for Surgical Implants (UNS R30075).
[45]. ASTM F562-13, Standard Specification for Wrought 35Cobalt-35Nickel-20Chromium-10Molybdenum Alloy for Surgical Implant Applications.
[46]. *D. F. Pascoe, J. Wimmer*, "A radiographic technique for the detection of internal defects in dental castings", in The Journal of Prosthetic Dentistry, **vol. 39**, no.2, Feb. 1978, pp. 150-157.
[47]. *R. K. Buddu, S. Shaikh, P.M. Raole, B. Sarkar*, "Weld defects analysis of 60 mm thick SS316L mock-ups of TIG and EB welds by Ultrasonic inspection for fusion reactor vacuum vessel applications", NDE2015 Proceedings, Nov. 2015.
[48]. N.P. Migoun, N.V. Delenkovsky, "The Ways of Penetrant Testing Applicability for Rough Surfaces". Proceedings of the 17th World Conference on Nondestructive Testing, Oct. 2008.